Molecular Crystals and Liquid Crystals
Publication details, including instructions for authors and subscription information:
http://www.informaworld.com/smpp/title~content=t713644168

Liquid-Crystalline Behavior and Structure of Charge-Transfer Complexes of Pyrene Derivatives with Four Linear Alkanoyloxy Substituents

Takuji Hirose[a]; Takuya Yumoto[a]; Kozue Matsumoto[a]; Satomi Mitsushio[a]; Osamu Kawakami[a]; Mikio Yasutake[a]
[a] Graduate School of Science and Engineering, Saitama University, Sakura, Saitama, Japan

First published on: 08 July 2010

To cite this Article Hirose, Takuji , Yumoto, Takuya , Matsumoto, Kozue , Mitsushio, Satomi , Kawakami, Osamu and Yasutake, Mikio(2010) 'Liquid-Crystalline Behavior and Structure of Charge-Transfer Complexes of Pyrene Derivatives with Four Linear Alkanoyloxy Substituents', Molecular Crystals and Liquid Crystals, 524: 1, 68 — 101
To link to this Article: DOI: 10.1080/15421406.2010.484613
URL: http://dx.doi.org/10.1080/15421406.2010.484613

Mol. Cryst. Liq. Cryst., Vol. 524: pp. 68–101, 2010

ISSN: 1542-1406 print/1563-5287 online
DOI: 10.1080/15421406.2010.484613

Taylor & Francis
Taylor & Francis Group

Liquid-Crystalline Behavior and Structure of Charge-Transfer Complexes of Pyrene Derivatives with Four Linear Alkanoyloxy Substituents

TAKUJI HIROSE, TAKUYA YUMOTO, KOZUE MATSUMOTO, SATOMI MITSUSHIO, OSAMU KAWAKAMI, AND MIKIO YASUTAKE

Graduate School of Science and Engineering, Saitama University, Sakura, Saitama, Japan

Pyrene derivatives (PCns) bearing four linear alkanoyloxy chains (n = 7, 9, 11, 15) were synthesized and shown to exhibit mesophases as a result of forming charge-transfer (CT) complexes with strongly electron-accepting 2,4,5,7-tetranitro-9-fluorenone (TeNF). The mesomorphic properties were investigated by polarizing optical microscopy (POM), differential scanning calorimetry (DSC), and variable-temperature X-ray diffraction (XRD) studies. The discotic lamellar phase was confirmed by XRD measurements, but no indication of intercalation of TeNF was observed. The CT complexation was supported by not only spectroscopic studies but the thermal behavior of the co-ground mixture.

Keywords Charge-transfer complex; lamellar structure; tetraalkanoyloxypyrenes; 2,4,5,7-tetranitro-9-fluorenone

Introduction

Discotic liquid crystals (DLCs) are usually composed of a rigid, flat core and several flexible peripheral chains, and their characteristic columnar structure is formed by stacking self-assembly. As a result, the columnar phases have one- or two-dimensional positional order, while retaining mobility. Accordingly, DLCs are expected to be used as readily processable and efficient one-dimensional organic charge-transport materials [1–7]. Large and highly symmetric discotic compounds are favorable for the formation of highly ordered columnar phases but tend to have high melting temperatures [4–7] and low solubility in common organic solvents [8]. In order to overcome these shortcomings, therefore, many researchers have investigated the molecular design and synthesis of new discotic compounds [9–13].

The induction of liquid-crystalline (LC) phases can be achieved by mixing different components, and charge-transfer (CT) complexation has been the most intensively investigated method [14–24]. Discotic compounds with electron-rich

Address correspondence to Takuji Hirose, Department of Applied Chemistry, Graduate School of Science and Engineering, Saitama University, 255 Shimo-okubo, Sakura, Saitama 338-8570, Japan. E-mail: hirose@apc.saitama-u.ac.jp

aromatic cores tend to form charge-transfer (CT) complexes with electron-deficient compounds, and CT complexation often allows non-liquid-crystalline compounds to form LC phases [14–18]. Therefore, CT interactions are an attractive subject from the perspective of not only organic electronics but also material engineering [19–24].

In our previous study [25], we reported LC phase formation of CT complexes between pyrene derivatives (PCns) bearing four linear alkanoyloxy chains ($n = 7$, 9, 11, 15) and 2,4,5,7-tetranitro-9-fluorenone (TeNF), and the columnar LC structures of the complexes were investigated by polarizing optical microscopy (POM) and differential scanning calorimetry (DSC). However, the details of the phase transitions and thermal behavior of the CT complexes remain to be studied. In this report, we conclude that the PCn-TeNF complexes form discotic lamellar mesophases, based on the results of XRD measurements and analysis of thermal complexation behavior.

Experimental

General

^{1}H NMR spectra were recorded on Bruker DPX-200 and AC-300P spectrometers (Molecular Analysis and Life Science Center (MALS), Saitama University, Saitama, Japan) using $CDCl_3$ as the solvent. The chemical shifts were reported in parts per million using tetramethylsilane as an internal standard. IR spectra were recorded on a JASCO FT/IR-400 spectrometer (Tokyo, Japan). UV-Vis spectra in a solid state were recorded by reflection method on a JASCO V-550 spectrophotometer with ISV-469 (Tokyo, Japan). Melting points were determined with a Mitamura Riken Kogyo MEL-TEMP instrument (Tokyo, Japan) and were reported uncorrected.

Phase transition temperatures were determined using a Mac Science DSC-6200 differential scanning calorimeter. A Nikon OPTIPHOT2-POL optical polarized microscope equipped with Mettler FP-82 hot stage and Mettler FP-90 central processor was used to verify thermal transitions and characterize anisotropic textures.

Single-crystal analysis of PC7 and PC9 obtained by recrystallization from AcOEt solution was carried out using a Bruker SMART APEX (MALS). X-ray intensities were measured up to $2\theta_{max} = 55.0^\circ$ using graphite-monochromated MoKα radiation ($\lambda = 0.71069$ Å). The crystal structures were determined by a direct method and refined by the full-matrix least-squares method using SHELXL97 [26,27]. On the other hand, X-ray diffraction (XRD) analysis of PC7-TeNF and PC11-TeNF was performed on quartz substrate (sample thickness 0.5 mm) using a Rigaku model Ultima III X-ray diffractometer with a monochromated CuKα radiation source (Tokyo, Japan).

Most of the reagents were purchased from Wako Pure Chemical Inc., Kanto Chemical Inc., Tokyo Kasei Kogyo Co., Aldrich Chemicals Co., (Tokyo, Japan) and were used as received except tetrahydrofuran, which was distilled from sodium benzophenone ketyl solution under nitrogen atmosphere after drying over NaOH.

1,3,6,8-Tetrachloropyrene and 3,8-dihydroxypyrene-1,6-quinone were prepared according to Vollmann *et al.*[28] and 2,4,5,7-tetranitrofluorenone was also followed from the literature [29].

1,3,6,8-Tetraalkanoyloxypyrenes (PCn)

1,3,6,8-Tetraalkanoyloxypyrenes were synthesized according to the literature [30] and the typical procedure is as follows for 1,3,6,8-tetra(octanoyloxy)pyrene

(PC7): Crude octanoyl chloride was prepared in a conventional way using octanoic acid and thionyl chloride and was used for the following reaction after removing thionyl chloride under reduced pressure. 3,8-Dihydroxypyrene-1,6-quinone (400 mg, 1.51 mmol), zinc dust (1.17 g, 17.7 mmol), 4-*N,N*-dimethylaminopyridine (2.27 g, 18.6 mmol), and the acid chloride were suspended in dry THF (30 mL) under nitrogen, and the mixture was stirred at room temperature for 17 h. After reducing the amount of THF, the mixture was diluted with chloroform, filtered and washed with 10% HCl *aq*. a few times, and the organic phase was dried over anhydrous sodium sulfate for 3 h. The solvent was removed under reduced pressure. The residue was purified by repeated silica-gel chromatography with chloroform, 2:1 mixture of toluene and hexane, and recrystallized from 2-propanol to obtain colorless needles (130 mg, 0.17 mmol, 11.2%). ^{1}H-NMR (300 MHz, $CDCl_3$, TMS) ppm: δ 8.06 (s, 4H, Ar*H*), 7.74 (s, 2H, Ar*H*), 2.80 (t, $J = 2.57$ Hz, 8H, CH_2), 1.91 (quint, 8H, CH_2), 1.52–1.28 (m, 32H, CH_2), 0.92 (t, $J = 2.33$ Hz, 12H, CH_3).

1,3,6,8-Tetra(decanoyloxy)pyrene (PC9): Yield 13.8%. ^{1}H-NMR (300 MHz, $CDCl_3$, TMS) ppm: δ 8.06 (s, 4H, Ar*H*), 7.74 (s, 2H, Ar*H*), 2.80 (t, $J = 2.45$ Hz, 8H, CH_2), 1.91 (quint, 8H, CH_2), 1.47–1.21 (m, 48H, CH_2), 0.90 (t, $J = 2.33$ Hz, 12H, CH_3).

1,3,6,8-Tetra(dodecanoyloxy)pyrene (PC11): Yield 23.2%. ^{1}H-NMR (300 MHz, $CDCl_3$, TMS) ppm: δ 8.06 (s, 4H, Ar*H*), 7.74 (s, 2H, Ar*H*), 2.80 (t, $J = 2.57$ Hz, 8H, CH_2), 1.91 (quint, 8H, CH_2), 1.48–1.23 (m, 64H, CH_2), 0.86 (t, $J = 2.20$ Hz, 12H, CH_3).

1,3,6,8-Tetra(hexadecanoyloxy)pyrene (PC15): Yield 18.5%. ^{1}H-NMR (300 MHz, $CDCl_3$, TMS) ppm: δ 8.06 (s, 4H, Ar*H*), 7.74 (s, 2H, Ar*H*), 2.79 (t, $J = 2.45$ Hz, 8H, CH_2), 1.90 (quint, 8H, CH_2), 1.42–1.17 (m, 96H, CH_2), 0.88 (t, $J = 2.33$ Hz, 12H, CH_3).

Results and Discussion

Phase Transitions of Pyrene Derivatives (PCn) and Crystal Structures of PC7 and PC9

Table 1 lists the thermal properties of the pyrene derivatives PCn ($n = 7$, 9, 11, 15) bearing four OCO(n-C_nH_{2n+1}) side chains. No PCn derivatives exhibited a mesophase.

A single crystal of PC7, as well as PC9, was obtained and analyzed by the direct method and the structures were refined by the full-matrix least-squares method (Appendix) [26,27]. Interestingly, the directions of the alkanoyloxy chains of PC7 and PC9 are different. All side chains of PC9 extend along the minor axis of the pyrene unit, and the molecular shape is tag-like. On the other hand, three side chains of PC7 extend along the major axis and the molecular shape is partly discoid as the other side chain bends with an opposite orientation (Fig. 1).

Phase Transitions and POM Observation of PCn-TeNF Complexes

It is known that mesophases can be induced from non-liquid-crystalline discotic molecules via CT interactions, and 2,4,7-trinitro-9-fluorenone (TNF) has been used as an electron acceptor for various electron-donor molecules [14–18]. Unfortunately, however, mixtures of TNF with PCn did not exhibit LC properties. It was assumed that the electron deficiency of TNF would be insufficient to form CT complexes with PCn. In order to examine this assumption, TeNF was synthesized [29] and mixtures with PCn were prepared in $CHCl_3$ solution [25]. The color of all mixtures turned reddish brown, suggesting the formation of CT complexes.

Table 1. Phase transitions of PCn determined by DSC[a]

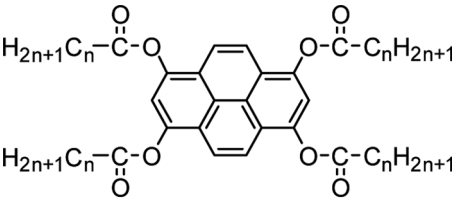

PCn

	Phase transition[b] temperature (°C) and enthalpy change (kJ mol^{-1})	
	Heating	Cooling
PC7	Cr 89 (39.1) I	I 75 (39.0) Cr
PC9	Cr 85 (40.5) I	I 67 (43.4) Cr
PC11	Cr 94 (46.9) I	I 71 (50.5) Cr
PC15	Cr 97 (57.5) I	I 82 (51.2) Cr

[a]Heating and cooling scan rates were 5°C min^{-1}.
[b]Abbreviations. Cr: Crystalline, I: Isotropic.

The thermal properties and phase transitions of various PCn-TeNF mixtures with known concentrations were investigated by DSC and POM, respectively. Figure 2 shows the results for PC7- and PC11-TeNF systems as the phase diagrams [31,32] and Table 2 lists the phase transition temperatures of all mixtures, as determined from DSC data for the first cooling curve obtained at a cooling rate of 5°C min^{-1}. It was found that simple tetraalkanoyloxypyrenes formed mesophases when highly electro-deficient TeNF was mixed in molar ratios of 15–65%, depending on side chain length [25]. A clear tendency of TeNF to separate was observed at higher concentrations, as has also been reported for some discotic compound-TNF systems [17,20,22,23]. PC11 formed an LC phase over the widest range of TeNF concentrations, but phase separation appeared at TeNF concentrations of ~40%. On the other hand, the LC phases of PC7 and PC9 were homogeneous up to TeNF concentrations of ~50%.

In order to determine the stable composition of the present charge-transfer complex, the relationship between TeNF concentration and the highest I-D_L transition

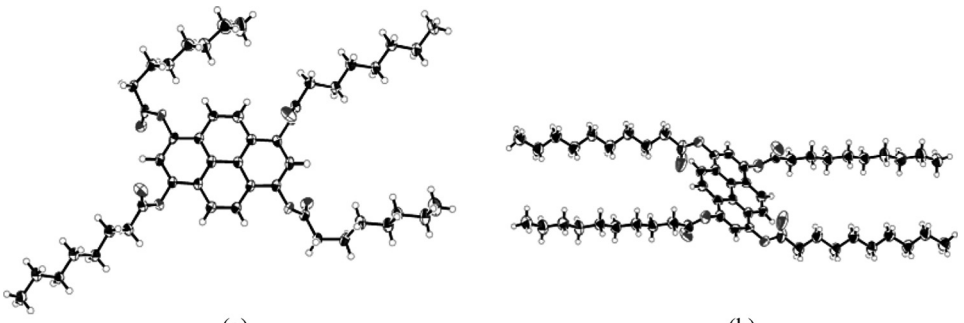

(a) (b)

Figure 1. Molecular structures of PC7 and PC9 solved by single-crystal X-ray analysis.

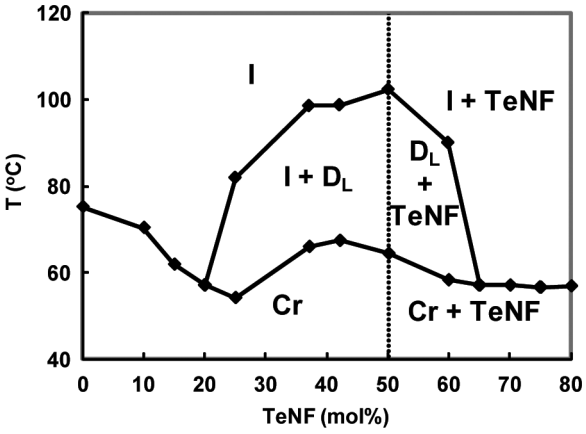

(a)

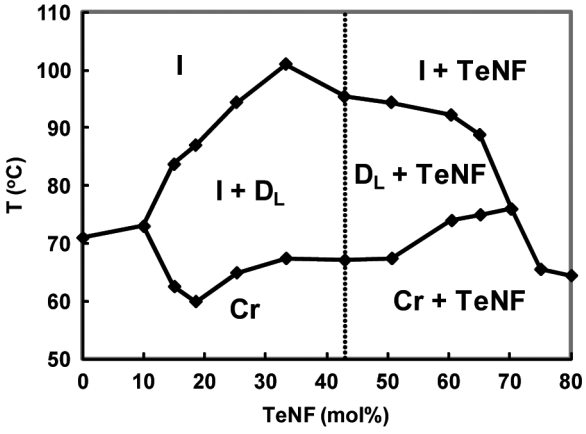

(b)

Figure 2. The binary phase diagrams for (a) PC7-TeNF and (b) PC11-TeNF systems.

temperature was plotted in Fig. 3. The composition gradually changed from 1:1 for PC7-TeNF and 2:1 for PC11- and PC15-TeNF systems, suggesting that the side chains hinder the interaction of TeNF. It should be noted that the widest temperature range of the D_L phase was attained at the same composition for each system, which supports the stability of the mesophase.

The LC phases formed during cooling of PCn-TeNF ($n = 7$–15, TeNF 33 mol%) had seaweed-like textures [33] and sometimes mosaic textures [34,35], thus, the phases were thought to be columnar (Fig. 4) [25]. In order to determine the mesophase structure, the complexes were investigated by variable-temperature XRD.

UV-Vis and IR Spectra of PCn-TeNF Complexes

The color change of PCn was investigated by comparing the UV-Vis spectra of PC11, TeNF, and PC11-TeNF (TeNF 33 mol%) in the solid state. As shown in Fig. 5, a new absorption band appeared in the range of 450–700 nm (λ_{max}: 570 nm), which was not observed in the spectrum of either PCn or TeNF. The

Table 2. Phase transitions of binary mixtures of PCn and TeNF as a function of molar ratio of TeNF, as determined by DSC[a] and POM in the cooling process

TeNF ratio (mol%)	Phase transition[b] temperature (°C)			
	PC7	PC9	PC11	PC15
0	I 75 Cr	I 67 Cr	I 71 Cr	I 82 Cr
15	I 60 Cr	I 66 Cr	I 84 D_L 63 Cr	I 75 Cr
20	I 57 Cr	I 91 D_L 65 Cr	I 87 D_L 60 Cr	I 83 D_L 74 Cr
25	I 82 D_L 54 Cr	—	I 94 D_L 65 Cr	I 89 D_L 75 Cr
30	—	—	—	I 93 D_L 75 Cr
33	I 90 D_L 67 Cr	I 105 D_L 65 Cr	I 101 D_L 67 Cr	I[c] 89 D_L[c]75 Cr
43	I 98 D_L 67 Cr	I 123 D_L 65 Cr	I[c] 95 D_L[c] 67 Cr	I[c] 89 D_L[c] 75 Cr
50	I[c] 102 D_L[c] 64 Cr	I[c] 100 D_L[c] 66 Cr	I[c] 94 D_L[c] 67 Cr	I[c] 81 D_L[c] 76 Cr
60	I[c] 90 D_L[c] 58 Cr	I[c] 96 D_L[c] 66 Cr	I[c] 92 D_L[c] 67 Cr	—
65	I[c] 57 Cr	I[c] 80 D_L[c] 64 Cr	I[c] 89 D_L[c] 67 Cr	—
70	I[c] 57 Cr	I[c] 70 Cr	I[c] 76 Cr	I[c] 77 Cr
80	I[c] 57 Cr	I[c] 65 Cr	I[c] 66 Cr	I[c] 76 Cr

[a]Cooling scan rate: 5°C min^{-1}.
[b]Abbreviations; Cr: Crystalline, I: Isotropic, D_L: Discotic lamellar.
[c]Phase separation of TeNF was observed.

spectrum is similar to the result reported for TNF complexes in solution [21]. In the present system, a slight color change was observed visually in the $CHCl_3$ solution, but this change was not clearly detected by the apparatus.

The charge-transfer complex is thought to form between the HOMO of electron-donating PC11 and the LUMO of electron-accepting TeNF. The energy levels were calculated by using MOPAC and the HOMO(PC11)–LUMO(TeNF) energy difference was 2.16 eV. The maximum absorption wavelength (570 nm) of the new absorption band, which corresponded to a transition energy of 2.21 eV, was in good agreement with the calculated energy difference.

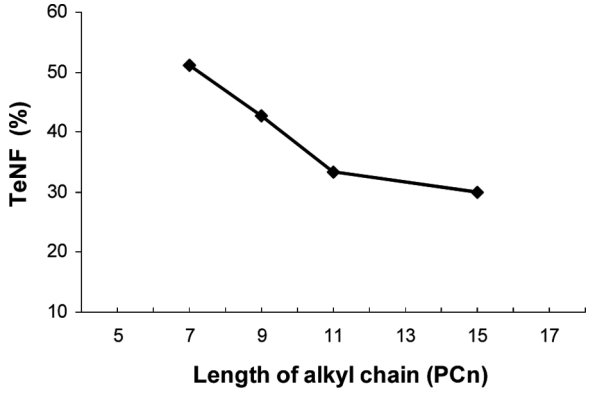

Figure 3. The relationship between the side chain length *n* and the TeNF content at the highest I-D_L transition temperature of the PCn-TeNF systems.

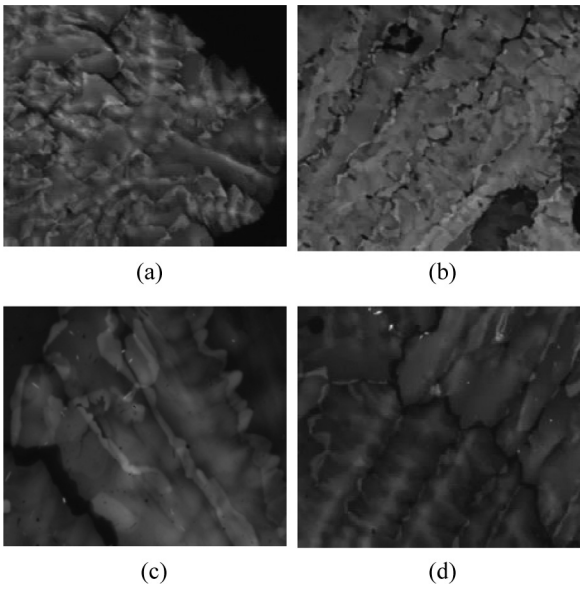

Figure 4. Optical texture of charge transfer mesophases of PCn-TeNF (TeNF 33 mol%). (a) PC7-TeNF at 85°C, (b) PC9-TeNF at 85°C, (c) PC11-TeNF at 90°C, and (d) PC15-TeNF at 85°C.

The CT interaction was also inferred from a comparison of the infrared (IR) spectra of PCn, TeNF, and PCn-TeNF. In the spectrum of PC7-TeNF (TeNF 33 mol%), for example, splitting or shifting of NO_2 absorption bands as well as other small changes were observed, as shown in Fig. 6. Similar results were obtained for the UV-Vis and IR spectra of all complexes investigated in this study.

XRD Study of PCn-TeNF

The X-ray diffraction patterns of PC7-TeNF (TeNF 33 mol%) at 75°C and PC11-TeNF (TeNF 33 mol%) at 75°C are shown in Figs. 7a and 7b, respectively.

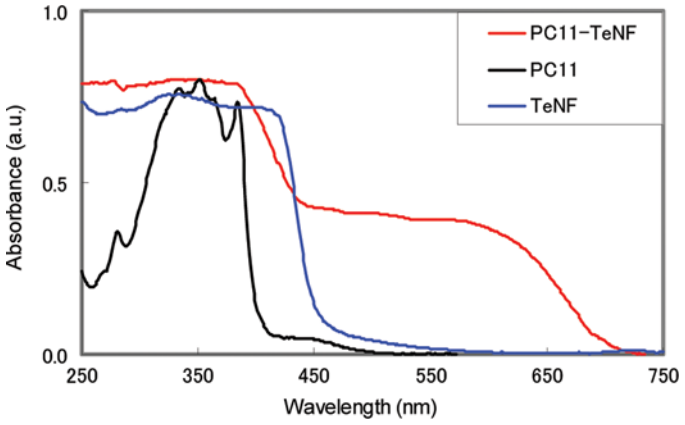

Figure 5. UV-Vis spectra of complexes of PC11-TeNF (TeNF 33 mol%) in the solid state.

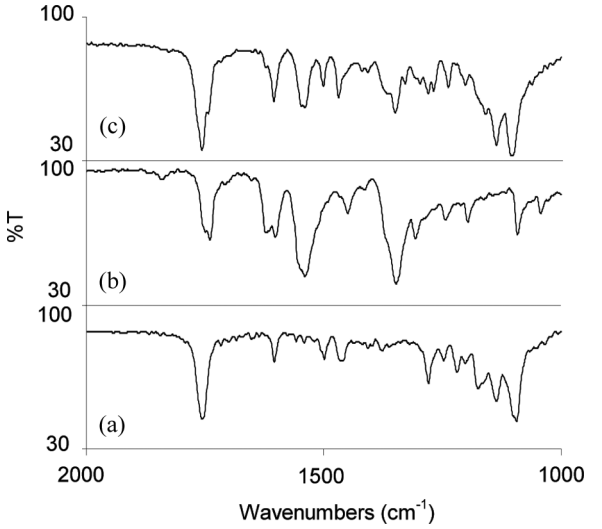

Figure 6. IR spectra of (a) PC7, (b) TeNF, and (c) PC7-TeNF (TeNF 33 mol%).

As shown in Fig. 7a, a strong sharp reflection at 18.5 Å and much less intense but sharp reflections at 9.29, 6.17, 4.63, and 3.08 Å were observed; the intensity of these peaks had a ratio of 1:1/2:1/3:1/4:1/6. Accordingly, these are assigned as one-dimensional peaks (d_{001}-d_{004}, d_{006}), which are typical of a lamellar phase (Table 3). In addition, a broad scattering halo was also observed at 4.37 Å, corresponding to the molten alkyl chains (h_{ch}). On the other hand, for PC11-TeNF (Fig. 7b), five sharp reflections were also observed at 22.8, 11.5, 7.68, 5.74, and 4.59 Å with a ratio of 1:1/2:1/3:1/4:1/5 to be assigned as d_{001}-d_{005}. A broad halo was again observed at 4.36 Å as h_{ch}, in good agreement with that of PC7-TeNF. Both first-order reflections, 18.5 Å for PC7-TeNF and 22.8 Å for PC11-TeNF, were shorter than the longer dimensions of PCn determined by single-crystal analysis of PC7 (24.98 Å) and by MM2 molecular modeling for PC11 (33.62 Å) [36]. Thus, the molecules are expected to be tilted in the layer, and the tilt angles were calculated to be 47.8° for PC7 and 42.6° for PC11 according to Ohta *et al.* [37,38].

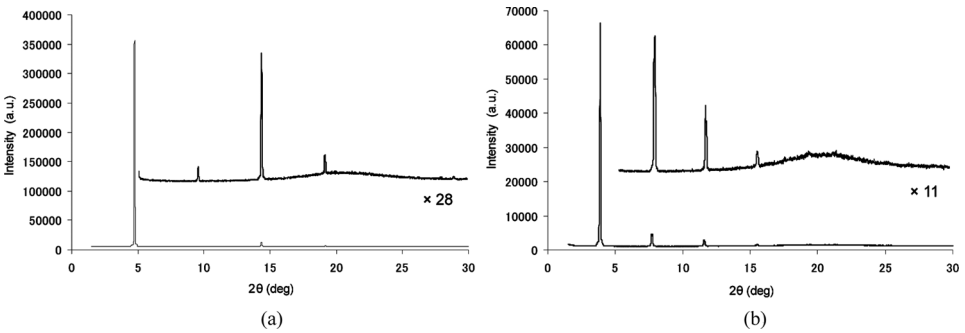

Figure 7. X-ray diffraction patterns of (a) PC7-TeNF (TeNF 33 mol%) at 75°C and (b) PC11-TeNF (TeNF 33 mol%) at 75°C.

Table 3. XRD data for liquid crystalline phases of PC7-TeNF (TeNF 33 mol%) at 75°C and PC11-TeNF (TeNF 33 mol%) at 75°C

Compound (mesophase)	Spacing/Å		Miller indices (h k l)	Tilt angle (°) $0 = \arcsin(d/l)^a$
	Observed	Calculated		
PC7-TeNF	18.6	18.6	(0 0 1)	$l = 22.87^b$
(TeNF 33 mol%)	9.29	9.29	(0 0 2)	
D_L at 75°C	6.17	6.20	(0 0 3)	$\theta = 47.82$
	4.63	4.65	(0 0 4)	
	3.08	3.10	(0 0 6)	
$d = 18.5$ Å	4.37	—	h_{ch}	
PC11-TeNF	22.8	22.8	(0 0 1)	$l = 33.62^c$
(TeNF 33 mol%)	11.4	11.4	(0 0 2)	
D_L at 75°C	7.64	7.58	(0 0 3)	$\theta = 42.59$
$d = 22.8$ Å	5.72	5.69	(0 0 4)	
	4.58	4.55	(0 0 5)	
	4.36	—	h_{ch}	

[a] l: Molecular length.
[b] Determined by single-crystal structure.
[c] Estimated by MM2.

There are many examples in which charge-transfer interactions between planar electron-rich and electron-deficient molecules allow LC phase formation including lamellar phases. However, the structural relationship between the components is still controversial. A majority of TNF complexes have been reported to be face-to-face 1:1 or 1:2 structures [18,39,40]. On the other hand, Gionis *et al.* reported the first CT complex lamellar phase between tetrasubstituted dithiapyranylidenes and TCNQ [41]. They concluded that the CT complex forms the lamellar structure via stacking of the donor molecules with TCNQ molecules filling the space between stacks. In addition, Kruglova *et al.* recently reported that TNF molecules are not sandwiched between hexaalkoxytriphenylene (HAT) molecules in the columnar phase but rather are located between the columns within the tails of HAT [42]. In the present PCn-TeNF systems, the stable composition ratio could not be determined for the D_L phase because it depended on n as shown in Table 1. At present, therefore, it is difficult to present unambiguously the columnar structure and location of TeNF [43].

Thermal Behavior of PCn-TeNF Complexes

Close POM observation of the PCn-TeNF complexes with high TeNF content revealed complex phase transitions as a result of thermal hysteresis. As an example, the PC11-TeNF (TeNF 50 mol%) complex prepared by concentration of the $CHCl_3$ solution was chosen for more detailed study. During the first heating process, the crystalline phase transitioned to the D_L phase at 110°C (Fig. 8a) and at 112°C crystalline fine needles (X) started to form up to 124°C (Fig. 8b) as the D_L phase

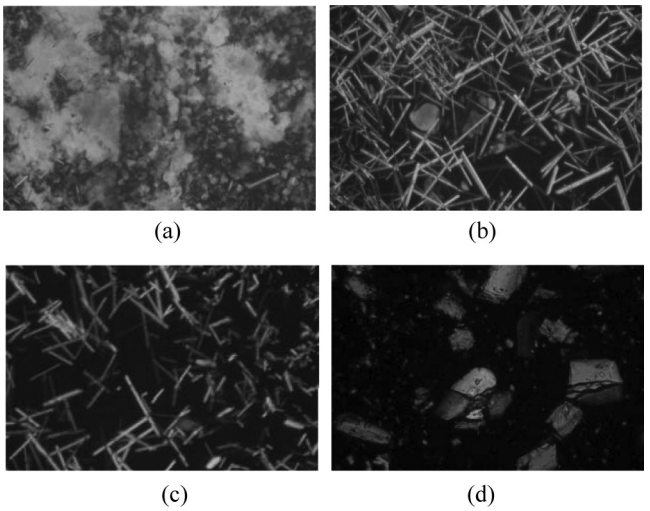

Figure 8. Effects of thermal annealing on phase changes of PC11-TeNF (TeNF 50 mol%) at heating rate of 10°C min^{-1} during first heating at (a) 110°C, (b) 124°C, and (c) 165°C. (d) Originally crystalline TeNF at 165°C.

disappeared. Though this new phase began to slowly melt soon after appearing, up to 165°C (Fig. 8c), originally crystalline TeNF (rectangular, Fig. 8d) did not change in this temperature range. This new phase was found to be irreproducible; that is, only the Cr-D_L-Iso phase transition is observed after the first cooling process. Similar transitions were observed for all PCn-TeNF (TeNF 50 mol%) systems. It seems that the new crystalline phase that is formed after the lamellar phase becomes isotropic, but the phase transition is not observed in the DSC measurement. Thus, the transition appears to be heterogeneous just as Lehmann *et al.* reported for metal complex-TNF systems [20] The phase transitions, as determined primarily by DSC, are summarized in Table 4.

Table 4. Phase transitions observed by POM for PC11-TeNF (TeNF 50 mol%) upon first heating

Temp. (°C)	85	112(124)	256
PCll-TeNF	Cr → D_{Ld} → Iso → Iso		Iso Iso
		a X *b* Iso	
TeNF			Cr $\xrightarrow{c}$ Cr

Heating scan rate was 5°C min^{-1}.
Abbreviations: Cr: Crystalline, D_L: Discotic lamellar,.
I: Isotropic, X: Undetermined.
[a]Gradually grows between 112°C and 124°C.
[b]Gradually melts between 124–165°C.
[c]Melts at 256°C but no transition is detected in the DSC measurement trace.

CT Complexation of PCn and TeNF Mixtures (PCn + TeNF) by Thermal Annealing

Thermal transition of PCn-TeNF complexes with high TeNF content suggested that the D_L phase ratio changes as a result of thermal annealing. In order to investigate the effects of annealing, a solid mixture of PC11 and TeNF, PC11 + TeNF, was prepared by co-grinding in a mortar [44]. The thermal behavior of PC11 + TeNF (TeNF 50 mol%) was observed by POM for the first heating process up to 180°C, which is above the melting point of PC11 but below the melting point of TeNF (255–257°C), as well as the first cooling process. The changes observed in the micrographs are shown in Fig. 9. Based on the Cr-D_L transition temperature of PC11-TeNF (TeNF 33 mol%) listed in Table 2, all images seen in Figs. 9a and 9b are expected to show crystalline TeNF, and the amount of TeNF decreases even below its melting point (170°C), as shown in Fig. 9b. These figures suggest that melted PC11 begins to interact with TeNF and form the CT complex spontaneously. In fact, in the first cooling process after annealing at 180°C, the seaweed-like texture of the D_L phase was observed at 95°C, as shown in Fig. 9c. The UV-Vis spectra of the PCn+TeNF before and after annealing at 180°C are shown in Fig. 10.

The spectrum of the mixture before annealing corresponds well with the sum of the spectra of PC11 and TeNF with a small absorption increase in the 450–700 nm range (Fig. 10). No color change was detected visually. After annealing below the melting point of TeNF, the spectrum of the reddish brown sample showed a broad absorption at 450–700 nm. All of the UV-Vis data clearly correspond to those of PC11-TeNF (cf. Fig. 5) and indicate that PCn and TeNF spontaneously form a complex in the liquid state due to their CT interaction.

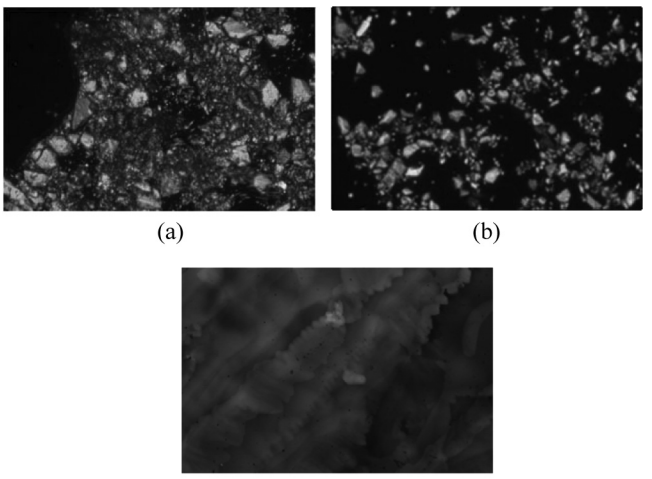

Figure 9. Optical texture change of the solid mixture of PC11 + TeNF (TeNF 50 mol%) before and after thermal annealing at 180°C. (a) At 94°C during first heating (before annealing), (b) at 170°C during first heating (before annealing), (c) at 95°C during first cooling (after annealing at 180°C).

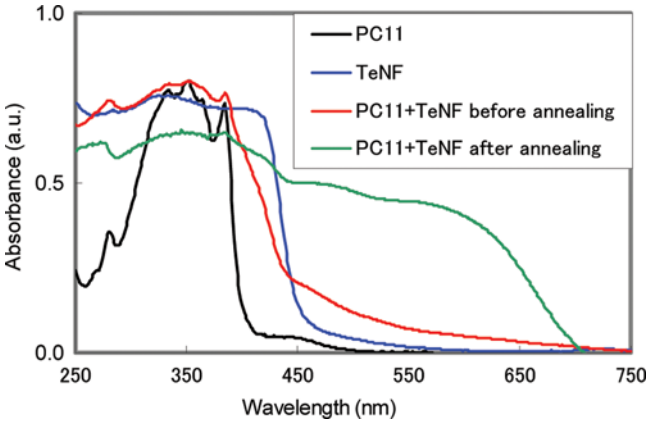

Figure 10. UV-Vis spectra of solid mixture PC11 + TeNF (TeNF 50 mol%) before and after first annealing at 180°C.

Conclusion

Crystalline pyrene derivatives bearing four linear $C_nH_{2n+1}CO_2$ groups (PCn: $n = 7$, 9, 11, 15) were synthesized, and the thermal properties of the complexes they formed with 2,4,5,7-tetranitro-9-fluorenone (TeNF) were investigated. From POM observations as well as DSC and XRD measurements, the complexes were shown to form lamellar mesophases. It was shown that the stronger charge-transfer interaction between PCn and TeNF, compared with that between PCn and 2,4,7-trinitro-9-fluorenone, was the cause of the mesophase induction. This accounted for not only the color change of PCn upon complexation but also the UV-Vis and IR spectra. Based on the layer distance and the weak reflection attributed to the stacking of the aromatic rings, the layer structure was assumed to consist of flat molecules tilted relative to the layer at an angle of 47.8° for PC7 and 42.6° for PC11, interacting with randomly distributed TeNF molecules. The CT interaction was also demonstrated by the thermally induced spontaneous complexation of mechanical mixtures of PC7 and TeNF; however, the structural relationship of the components in these mixtures remains as a topic for further investigation.

Acknowledgments

The authors thank Professor Kazuchika Ohta of Shinshu University for his useful discussion and suggestions.

References

[1] Cammidge, A. N., & Bushby, R. J. (1998). Synthesis and Structural Features. In: *Handbook of Liquid Crystals*, Demus, D., Goodby, J., Gray, G. W., Spiess, H.-W., & Vill, V. (Eds.), Wiley-VCH: New, USA, Vol. 2B, Chapter VII, 693.

[2] Mori, H., Itoh, Y., Nishiura, Y., Nakamura, T., & Shinagawa, Y. (1997). *Jpn. J. Appl. Phys.*, *36*, 143.

[3] Kamada, K., Watanabe, J., Arakawa, K., & Kozono, H. (1995). Liquid Crystal Display. *European Patent Application*, 646829 A1.

[4] van de Craats, A. M., Warman, J. M., Fechtenkötter, A., Brand, J. D., Harbison, M. A., & Müllen, K. (1999). *Adv. Mater.*, *11*, 1469.
[5] Adam, D., Schuhmacher, P., Simmerer, J., Häussling, L., Siemensmeyer, K., Etzbachi, K. H., Ringsdorf, H., & Haarer, D. (1994). *Nature*, *371*, 141.
[6] Boden, N., & Movaghar, B. (1998). Application Properties of Columnar Discotic Liquid Crystals. In: *Handbook of Liquid Crystals*, Demus, D., Goodby, J., Gray, G. W., Spiess, H.-W., & Vill, V. (Eds.), Wiley-VCH: New York, USA, Vol. 2B, Chapter IX, 781.
[7] Warman, J. M., & Schouten, P. G. (1995). *J. Phys. Chem.*, *99*, 17181.
[8] Mullen, K., Spiess, H. W., Fechtenkotter, A., Saalwachter, K., & Harbison, M. A. (1999). *Angew. Chem. Int. Ed. Engl.*, *38*, 3039.
[9] Dieter, A., Peter, S., Juergen, S., Lukas, H., Wolfgang, P., Karl, S., Heinz, E. K., Helmut, R., & Dietrich, H. (1995). *Adv. Mater.*, *7*, 276.
[10] Krishnan, K., & Balagurusamy, V. S. K. (2001). *Liq. Cryst.*, *28*, 321.
[11] Rego, J. A., Kumar, S., & Ringsdorf, H. (1996). *Chem. Mater.*, *8*, 1402.
[12] Kouwer, P. H. J., Jager, W. F., Mijs, W. J., & Picken, S. J. (2004). *Mol. Cryst. Liq. Cryst.*, *411*, 305.
[13] Hassheider, T., Benning, S. A., Kitzerow, H.-S., Achard, M.-F., & Bock, H. (2001). *Angew. Chem. Int. Ed. Engl.*, *40*, 2060.
[14] Kumar, S., Takezoe, H., & Rao, D. S. S. (2008). *Bull. Chem. Soc. Jpn.*, *81*, 163.
[15] Seung, J. L., & Chang, J. Y. (2003). *Tetrahedron Lett.*, *44*, 7493.
[16] Kamikawa, Y., & Kato, T. (2006). *Org. Lett.*, *8*, 2463.
[17] Singer, D., Liebmann, A., Praefcke, K., & Wendorff, J. H. (1993). *Liq. Cryst.*, *3*, 785.
[18] Praefcke, K., Singer, D., Kohne, B., Ebert, M., Liebmann, A., & Wendorff, J. H. (1991). *Liq. Cryst.*, *10*, 147.
[19] Stepien, M., Donnio, B., & Sesler, J. L. (2007). *Angew. Chem. Int. Ed. Engl.*, *46*, 1431.
[20] Lehmann, M., Sierra, T., Barbera, J., Serrano, J. L., & Parker, R. (2002). *J. Mater. Chem.*, *12*, 1342.
[21] Markovitsi, D., Bengs, H., & Ringsdorf, H. (1992). *J. Chem. Soc. Faraday Trans.*, *88*, 1275.
[22] Bengs, H., Ebert, M., Karthaus, O., Kohne, B., Praefcke, K., Ringsdorf, H., Wendorff, J. H., & Wüstefeld, R. (1990). *Adv. Mater.*, *2*, 141.
[23] Ringsdorf, H., Wüstefeld, R., Zerta, E., Ebert, M., & Wendorff, J. H. (1989). *Angew. Chem. Int. Ed. Engl.*, *28*, 914.
[24] Janietz, D. (1996). *Chem. Commun.*, *6*, 713.
[25] Hirose, T., Kawakami, O., & Yasutake, M. (2006). *Mol. Cryst. Liq. Cryst.*, *45*, 65.
[26] Altomare, A., Burla, M. C., Camalli, M., Cascarano, G. L., Giacovazzo, C., Guagliardi, A., Moliterni, A. G. G., Polidori, G., & Spagna, R. (1999). *J. Appl. Cryst.*, *32*, 115.
[27] Sheldrick, G. M. (1997). *SHELEXL97: Program for the Refinement of Crystal Structures*, University of Göttingen: Germany.
[28] Vollmann, H., Becker, H., Correll, M., & Streeck, H. (1937). *Liebigs Ann. Chem.*, *1*, 531.
[29] Newman, M. S., & Boden, H. (1962). *Organic Syntheses*, *42*, 95.
[30] Bock, H., & Helfrich, W. (1995). *Liq. Cryst.*, *18*, 707.
[31] Matsunaga, Y., Saito, G., & Sakai, N. (1974). *Bull. Chem. Soc. Jpn.*, *47*, 2873.
[32] Fletcher, I. D., Guillon, D., Heinrich, B., Omenat, A., & Serrano, J. L. (1997). *Liq. Cryst.*, *23*, 51.
[33] Serrette, A. G., Lai, C. K., & Swager, T. M. (1994). *Chem. Mater.*, *6*, 2252.
[34] Ito, S., Ando, M., Nomura, A., Morita, N., Kabuto, C., Mukai, H., Ohta, K., Kawakami, J., Yoshizawa, A., & Tajiri, A. (2005). *J. Org. Chem.*, *70*, 3939.
[35] Ohta, K., Takenaka, O., Morizumi, Y., Fujimoto, T., & Yamamoto, I. (1991). *Mol. Cryst. Liq. Cryst.*, *195*, 135.
[36] MM2 calculations were performed with the MOPAC 2002 Version 2.5.3 of CAChe Version 7.5.0.85.
[37] Ohta, K., Muroki, H., Takagi, A., Hatada, K., Ema, H., Yamamoto, I., & Matsuzaki, K. (1986). *Mol. Cryst. Liq. Cryst.*, *140*, 131.

[38] Shimizu, Y., Miya, M., Nagata, A., Ohta, K., Matsumura, A., Yamamoto, I., & Kusubayashi, S. (1991). *Chem. Lett.*, 25.
[39] Praefcke, K., Singer, D., Kohne, B., Ebert, M., Liebmann, A., & Wendorff, J. H. (1991). *Liq. Cryst.*, *10*, 147.
[40] Bengs, H., Renkel, R., Ringsdorf, H., Baehr, C., Ebert, M., & Wendorff, J. H. (1991). *Makromol. Chem. Rapid Comm.*, *12*, 439.
[41] Davidson, P., Levelut, A. M., Strzelecka, H., & Gionis, V. (1983). *J. Phys. Lett.*, *44*, L-823.
[42] Kruglova, O., Mendes, E., Yildirim, Z., Wübbenhorst, M., Mulder, F. M., Stride, J. A., Picken, S. J., & Kearley, G. J. (2007). *Chem. Phys. Chem.*, *8*, 1338.
[43] Hegmann, T., Kain, J., Diele, S., Pelzl, G., & Tschierske, C. (2001). *Angew. Chem. Int. Ed.*, *40*, 887.
[44] Kuroda, R., Imai, Y., & Tajima, N. (2002). *Chem. Commun.*, 2848.

Appendix

Table A1. Single-crystal analysis data of PC7 and PC9

	PC7	PC9
Formula	$C_{48}H_{66}O_8$	$C_{56}H_{82}O_8$
Formula weight	771.01	883.22
Crystal color	Colorless	Colorless
Crystal description	Plate	Plate
Crystal size (mm)	$0.39 \times 0.10 \times 0.05$	$0.28 \times 0.11 \times 0.09$
Crystal system	Triclinic	Triclinic
Space group	P-1	P-1
	$a = 9.5114(19)$ Å $\alpha = 75.64(3)^\circ$	$a = 15.674(2)$ Å $\alpha = 91.844(5)^\circ$
	$b = 12.281(3)$ Å $\beta = 80.61(3)^\circ$	$b = 16.853(3)$ Å $\beta = 95.549(5)^\circ$
	$c = 19.810(4)$ Å $\gamma = 77.68(3)^\circ$	$c = 5.4425(6)$ Å $\gamma = 62.361(3)^\circ$
V (Å^3)	2175.3(8)	1267.5(3)
Z	2	1
T (K)	123(2)	123(2)
D_{calc} (Mg/cm^3)	1.177	1.157
$F(000)$	836	482
Reflections collected	9014	4276
Refinement method	Full-matrix least-squares on	
No. of parameters	509	291
Goodness-of-fitting on F^2	0.938	1.379
Final R indices [I > 2s(I)]	$R_1 = 0.0709$, $wR_2 = 0.1942$,	$R_1 = 0.1088$, $wR_2 = 0.2994$
R indices (all data)	$R_1 = 0.1735$, $wR_2 = 0.2306$	$R_1 = 0.2255$, $wR_2 = 0.4042$
$(\Delta\rho)_{max}$	0.321 e.Å^{-3}	0.413 e.Å^{-3}
$(\Delta\rho)_{min}$	-0.597 e.Å^{-3}	-0.433 e.Å^{-3}

Crystallographic data of PC7 and PC9 have been deposited with the Cambridge Crystallographic Data Center: Deposition numbers CCDC-XXXXX and CCDC-YYYYY, respectively.

Table A2. Atomic coordinates ($\times 10^4$) and equivalent isotropic displacement parameters ($Å^2 \times 10^3$) for PC7. U(eq) is defined as one third of the trace of the orthogonalized U^{ij} tensor

	x	*y*	*z*	U(eq)
C(1)	6182(4)	1160(3)	3616(2)	31(1)
C(2)	6163(4)	118(3)	4044(2)	29(1)
C(3)	6869(4)	−207(3)	4675(2)	26(1)
C(4)	6831(4)	−1241(3)	5145(2)	28(1)
C(5)	7479(4)	−1552(3)	5758(2)	29(1)
C(6)	8200(4)	−784(3)	5899(2)	27(1)
C(7)	8306(4)	277(3)	5457(2)	26(1)
C(8)	9098(4)	1066(3)	5592(2)	29(1)
C(9)	9164(4)	2086(3)	5137(2)	29(1)
C(10)	8448(4)	2427(3)	4519(2)	27(1)
C(12)	8431(4)	3483(3)	4056(2)	29(1)
C(12)	7649(4)	3823(3)	3484(2)	30(1)
C(13)	6905(4)	3068(3)	3351(2)	28(1)
C(14)	6918(4)	1967(3)	3761(2)	28(1)
C(15)	7620(4)	568(3)	4831(2)	26(1)
C(16)	7662(4)	1661(3)	4367(2)	25(1)
O(1)	5975(3)	−1956(2)	5020(1)	31(1)
O(2)	7929(3)	−3326(2)	4908(2)	36(1)
O(3)	8957(3)	−1096(2)	6496(1)	30(1)
O(4)	6911(3)	−1359(3)	7226(2)	50(1)
O(5)	9167(3)	4257(2)	4205(1)	31(1)
O(6)	10,578(3)	4313(3)	3171(2)	42(1)
O(7)	6115(3)	3421(2)	2764(1)	33(1)
O(8)	4159(3)	4022(3)	3471(2)	56(1)
C(17)	6642(5)	−3017(3)	4925(2)	32(1)
C(18)	5568(4)	−3673(3)	4820(2)	33(1)
C(19)	4707(4)	−3062(4)	4211(2)	36(1)
C(20)	5650(4)	−2790(4)	3517(2)	38(1)
C(21)	4839(5)	−2119(4)	2905(2)	48(1)
C(22)	5838(5)	−1850(4)	2221(2)	52(1)
C(23)	5083(6)	−1174(5)	1605(3)	65(2)
C(24)	6096(7)	−935(5)	926(3)	72(2)
C(25)	8193(5)	−1425(3)	7137(2)	31(1)
C(26)	9194(4)	−1846(4)	7695(2)	34(1)
C(27)	8393(5)	−2251(4)	8411(2)	38(1)
C(28)	9315(4)	−2631(4)	9016(2)	35(1)
C(29)	8498(5)	−3193(4)	9694(2)	38(1)
C(30)	9326(5)	−3574(4)	10,328(2)	36(1)
C(31)	8505(5)	−4239(4)	10,963(2)	41(1)
C(32)	9317(5)	−4645(4)	11,606(2)	50(1)
C(33)	10,229(4)	4646(3)	3703(2)	30(1)
C(34)	10,881(5)	5493(3)	3928(2)	35(1)

(*Continued*)

Table A2. Continued

	x	*y*	*z*	U(eq)
C(35)	11,147(4)	6514(3)	3335(2)	37(1)
C(36)	9763(5)	7319(4)	3122(2)	42(1)
C(37)	10,025(5)	8418(4)	2594(2)	46(1)
C(38)	10,644(6)	8278(4)	1860(2)	49(1)
C(39)	10,857(6)	9398(4)	1353(2)	52(1)
C(40)	11,494(6)	9288(5)	615(3)	68(2)
C(41)	4684(4)	3900(3)	2896(2)	33(1)
C(42)	3951(4)	4213(3)	2245(2)	32(1)
C(43)	4567(5)	5133(4)	1676(2)	37(1)
C(44)	3722(4)	5524(4)	1041(2)	37(1)
C(45)	4384(5)	6366(4)	446(2)	36(1)
C(46)	3553(5)	6800(4)	−191(2)	37(1)
C(47)	4236(5)	7660(4)	−769(2)	40(1)
C(48)	3369(5)	8146(4)	−1393(2)	52(1)

Table A3. Bond lengths (Å) and angles (°) for PC7

C(1)–C(2)	1.350(6)
C(1)–C(14)	1.435(6)
C(1)–H(1)	0.9300
C(2)–C(3)	1.444(5)
C(2)–H(2)	0.9300
C(3)–C(4)	1.380(6)
C(3)–C(15)	1.421(5)
C(4)–C(5)	1.383(5)
C(4)–O(1)	1.406(5)
C(5)–C(6)	1.380(5)
C(5)–H(3)	0.9300
C(6)–C(7)	1.392(6)
C(6)–O(3)	1.414(4)
C(7)–C(15)	1.427(5)
C(7)–C(8)	1.442(5)
C(8)–C(9)	1.357(6)
C(8)–H(4)	0.9300
C(9)–C(10)	1.425(5)
C(9)–H(5)	0.9300
C(10)–C(11)	1.389(6)
C(10)–C(16)	1.431(5)
C(11)–C(12)	1.385(5)
C(11)–O(5)	1.404(5)
C(12)–C(13)	1.376(6)
C(12)–H(6)	0.9300
C(13)–C(14)	1.393(6)

(*Continued*)

Table A3. Continued

C(13)–O(7)	1.414(4)
C(14)–C(16)	1.422(5)
C(15)–C(16)	1.431(5)
O(1)–C(17)	1.365(4)
O(2)–C(17)	1.199(5)
O(3)–C(25)	1.369(5)
O(4)–C(25)	1.191(5)
O(5)–C(33)	1.371(5)
O(6)–C(33)	1.195(5)
O(7)–C(41)	1.374(5)
O(8)–C(41)	1.198(5)
C(17)–C(18)	1.497(6)
C(18)–C(19)	1.517(5)
C(18)–H(7)	0.9700
C(18)–H(8)	0.9700
C(19)–C(20)	1.519(6)
C(19)–H(9)	0.9700
C(19)–H(10)	0.9700
C(20)–C(21)	1.511(6)
C(20)–H(11)	0.9700
C(20)–H(12)	0.9700
C(21)–C(22)	1.531(6)
C(21)–H(13)	0.9700
C(21)–H(14)	0.9700
C(22)–C(23)	1.492(6)
C(22)–H(15)	0.9700
C(22)–H(16)	0.9700
C(23)–C(24)	1.524(7)
C(23)–H(17)	0.9700
C(23)–H(18)	0.9700
C(24)–H(19)	0.9600
C(24)–H(20)	0.9600
C(24)–H(21)	0.9600
C(25)–C(26)	1.499(5)
C(26)–C(27)	1.517(6)
C(26)–H(22)	0.9700
C(26)–H(23)	0.9700
C(27)–C(28)	1.521(5)
C(27)–H(24)	0.9700
C(27)–H(25)	0.9700
C(28)–C(29)	1.520(6)
C(28)–H(26)	0.9700
C(28)–H(27)	0.9700
C(29)–C(30)	1.514(6)
C(29)–H(28)	0.9700

(*Continued*)

Table A3. Continued

C(29)–H(29)	0.9700
C(30)–C(31)	1.517(6)
C(30)–H(30)	0.9700
C(30)–H(31)	0.9700
C(31)–C(32)	1.520(6)
C(31)–H(32)	0.9700
C(31)–H(33)	0.9700
C(32)–H(34)	0.9600
C(32)–H(35)	0.9600
C(32)–H(36)	0.9600
C(33)–C(34)	1.504(6)
C(34)–C(35)	1.525(6)
C(34)–H(37)	0.9700
C(34)–H(38)	0.9700
C(35)–C(36)	1.519(5)
C(35)–H(39)	0.9700
C(35)–H(40)	0.9700
C(36)–C(37)	1.528(6)
C(36)–H(41)	0.9700
C(36)–H(42)	0.9700
C(37)–C(38)	1.514(6)
C(37)–H(43)	0.9700
C(37)–H(44)	0.9700
C(38)–C(39)	1.520(6)
C(38)–H(45)	0.9700
C(38)–H(46)	0.9700
C(39)–C(40)	1.517(6)
C(39)–H(47)	0.9700
C(39)–H(48)	0.9700
C(40)–H(49)	0.9600
C(40)–H(50)	0.9600
C(40)–H(51)	0.9600
C(41)–C(42)	1.494(5)
C(42)–C(43)	1.525(6)
C(42)–H(52)	0.9700
C(42)–H(53)	0.9700
C(43)–C(44)	1.524(5)
C(43)–H(54)	0.9700
C(43)–H(55)	0.9700
C(44)–C(45)	1.512(6)
C(44)–H(56)	0.9700
C(44)–H(57)	0.9700
C(45)–C(46)	1.521(6)
C(45)–H(58)	0.9700
C(45)–H(59)	0.9700

(*Continued*)

Table A3. Continued

C(46)–C(47)	1.517(6)
C(46)–H(60)	0.9700
C(46)–H(61)	0.9700
C(47)–C(48)	1.523(6)
C(47)–H(62)	0.9700
C(47)–H(63)	0.9700
C(48)–H(64)	0.9600
C(48)–H(65)	0.9600
C(48)–H(66)	0.9600
C(2)–C(1)–C(14)	121.7(4)
C(2)–C(1)–H(1)	119.1
C(14)–C(1)–H(1)	119.1
C(1)–C(2)–C(3)	120.3(4)
C(1)–C(2)–H(2)	119.8
C(3)–C(2)–H(2)	119.8
C(4)–C(3)–C(15)	117.9(4)
C(4)–C(3)–C(2)	122.7(4)
C(15)–C(3)–C(2)	119.4(4)
C(3)–C(4)–C(5)	123.2(4)
C(3)–C(4)–O(1)	117.4(4)
C(5)–C(4)–O(1)	119.1(4)
C(6)–C(5)–C(4)	117.8(4)
C(6)–C(5)–H(3)	121.1
C(4)–C(5)–H(3)	121.1
C(5)–C(6)–C(7)	123.4(4)
C(5)–C(6)–O(3)	119.7(4)
C(7)–C(6)–O(3)	116.8(4)
C(6)–C(7)–C(15)	117.1(4)
C(6)–C(7)–C(8)	123.5(4)
C(15)–C(7)–C(8)	119.3(4)
C(9)–C(8)–C(7)	120.5(4)
C(9)–C(8)–H(4)	119.7
C(7)–C(8)–H(4)	119.7
C(8)–C(9)–C(10)	121.9(4)
C(8)–C(9)–H(5)	119.1
C(10)–C(9)–H(5)	119.1
C(11)–C(10)–C(9)	123.8(4)
C(11)–C(10)–C(16)	117.1(4)
C(9)–C(10)–C(16)	119.1(4)
C(12)–C(11)–C(10)	122.7(4)
C(12)–C(11)–O(5)	119.2(4)
C(10)–C(11)–O(5)	118.0(4)
C(13)–C(12)–C(11)	118.8(4)
C(13)–C(12)–H(6)	120.6
C(11)–C(12)–H(6)	120.6

(*Continued*)

Table A3. Continued

C(12)–C(13)–C(14)	122.8(4)
C(12)–C(13)–O(7)	118.4(4)
C(14)–C(13)–O(7)	118.8(4)
C(13)–C(14)–C(16)	117.2(4)
C(13)–C(14)–C(1)	123.4(4)
C(16)–C(14)–C(1)	119.4(4)
C(3)–C(15)–C(7)	120.5(4)
C(3)–C(15)–C(16)	120.0(4)
C(7)–C(15)–C(16)	119.5(4)
C(14)–C(16)–C(15)	119.2(4)
C(14)–C(16)–C(10)	121.2(4)
C(15)–C(16)–C(10)	119.6(4)
C(17)–O(1)–C(4)	118.0(3)
C(25)–O(3)–C(6)	117.7(3)
C(33)–O(5)–C(11)	117.2(3)
C(41)–O(7)–C(13)	115.5(3)
O(2)–C(17)–O(1)	122.3(4)
O(2)–C(17)–C(18)	126.8(4)
O(1)–C(17)–C(18)	110.9(4)
C(17)–C(18)–C(19)	113.2(3)
C(17)–C(18)–H(7)	108.9
C(19)–C(18)–H(7)	108.9
C(17)–C(18)–H(8)	108.9
C(19)–C(18)–H(8)	108.9
H(7)–C(18)–H(8)	107.8
C(18)–C(19)–C(20)	113.3(3)
C(18)–C(19)–H(9)	108.9
C(20)–C(19)–H(9)	108.9
C(18)–C(19)–H(10)	108.9
C(20)–C(19)–H(10)	108.9
H(9)–C(19)–H(10)	107.7
C(21)–C(20)–C(19)	115.0(3)
C(21)–C(20)–H(11)	108.5
C(19)–C(20)–H(11)	108.5
C(21)–C(20)–H(12)	108.5
C(19)–C(20)–H(12)	108.5
H(11)–C(20)–H(12)	107.5
C(20)–C(21)–C(22)	113.0(4)
C(20)–C(21)–H(13)	109.0
C(22)–C(21)–H(13)	109.0
C(20)–C(21)–H(14)	109.0
C(22)–C(21)–H(14)	109.0
H(13)–C(21)–H(14)	107.8
C(23)–C(22)–C(21)	114.7(4)
C(23)–C(22)–H(15)	108.6

(*Continued*)

Table A3. Continued

C(21)–C(22)–H(15)	108.6
C(23)–C(22)–H(16)	108.6
C(21)–C(22)–H(16)	108.6
H(15)–C(22)–H(16)	107.6
C(22)–C(23)–C(24)	113.8(5)
C(22)–C(23)–H(17)	108.8
C(24)–C(23)–H(17)	108.8
C(22)–C(23)–H(18)	108.8
C(24)–C(23)–H(18)	108.8
H(17)–C(23)–H(18)	107.7
C(23)–C(24)–H(19)	109.5
C(23)–C(24)–H(20)	109.5
H(19)–C(24)–H(20)	109.5
C(23)–C(24)–H(21)	109.5
H(19)–C(24)–H(21)	109.5
H(20)–C(24)–H(21)	109.5
O(4)–C(25)–O(3)	123.7(4)
O(4)–C(25)–C(26)	126.1(4)
O(3)–C(25)–C(26)	110.3(3)
C(25)–C(26)–C(27)	111.9(4)
C(25)–C(26)–H(22)	109.2
C(27)–C(26)–H(22)	109.2
C(25)–C(26)–H(23)	109.2
C(27)–C(26)–H(23)	109.2
H(22)–C(26)–H(23)	107.9
C(26)–C(27)–C(28)	115.4(4)
C(26)–C(27)–H(24)	108.4
C(28)–C(27)–H(24)	108.4
C(26)–C(27)–H(25)	108.4
C(28)–C(27)–H(25)	108.4
H(24)–C(27)–H(25)	107.5
C(29)–C(28)–C(27)	112.3(4)
C(29)–C(28)–H(26)	109.1
C(27)–C(28)–H(26)	109.1
C(29)–C(28)–H(27)	109.1
C(27)–C(28)–H(27)	109.1
H(26)–C(28)–H(27)	107.9
C(30)–C(29)–C(28)	115.8(4)
C(30)–C(29)–H(28)	108.3
C(28)–C(29)–H(28)	108.3
C(30)–C(29)–H(29)	108.3
C(28)–C(29)–H(29)	108.3
H(28)–C(29)–H(29)	107.4
C(29)–C(30)–C(31)	112.8(4)
C(29)–C(30)–H(30)	109.0

(*Continued*)

Table A3. Continued

C(31)–C(30)–H(30)	109.0
C(29)–C(30)–H(31)	109.0
C(31)–C(30)–H(31)	109.0
H(30)–C(30)–H(31)	107.8
C(30)–C(31)–C(32)	114.0(4)
C(30)–C(31)–H(32)	108.7
C(32)–C(31)–H(32)	108.7
C(30)–C(31)–H(33)	108.7
C(32)–C(31)–H(33)	108.7
H(32)–C(31)–H(33)	107.6
C(31)–C(32)–H(34)	109.5
C(31)–C(32)–H(35)	109.5
H(34)–C(32)–H(35)	109.5
C(31)–C(32)–H(36)	109.5
H(34)–C(32)–H(36)	109.5
H(35)–C(32)–H(36)	109.5
O(6)–C(33)–O(5)	122.7(4)
O(6)–C(33)–C(34)	126.4(4)
O(5)–C(33)–C(34)	110.9(3)
C(33)–C(34)–C(35)	113.0(4)
C(33)–C(34)–H(37)	109.0
C(35)–C(34)–H(37)	109.0
C(33)–C(34)–H(38)	109.0
C(35)–C(34)–H(38)	109.0
H(37)–C(34)–H(38)	107.8
C(36)–C(35)–C(34)	113.4(4)
C(36)–C(35)–H(39)	108.9
C(34)–C(35)–H(39)	108.9
C(36)–C(35)–H(40)	108.9
C(34)–C(35)–H(40)	108.9
H(39)–C(35)–H(40)	107.7
C(35)–C(36)–C(37)	113.6(4)
C(35)–C(36)–H(41)	108.8
C(37)–C(36)–H(41)	108.8
C(35)–C(36)–H(42)	108.8
C(37)–C(36)–H(42)	108.8
H(41)–C(36)–H(42)	107.7
C(38)–C(37)–C(36)	115.5(4)
C(38)–C(37)–H(43)	108.4
C(36)–C(37)–H(43)	108.4
C(38)–C(37)–H(44)	108.4
C(36)–C(37)–H(44)	108.4
H(43)–C(37)–H(44)	107.5
C(37)–C(38)–C(39)	113.3(4)
C(37)–C(38)–H(45)	108.9

(*Continued*)

Table A3. Continued

C(39)–C(38)–H(45)	108.9
C(37)–C(38)–H(46)	108.9
C(39)–C(38)–H(46)	108.9
H(45)–C(38)–H(46)	107.7
C(40)–C(39)–C(38)	114.7(4)
C(40)–C(39)–H(47)	108.6
C(38)–C(39)–H(47)	108.6
C(40)–C(39)–H(48)	108.6
C(38)–C(39)–H(48)	108.6
H(47)–C(39)–H(48)	107.6
C(39)–C(40)–H(49)	109.5
C(39)–C(40)–H(50)	109.5
H(49)–C(40)–H(50)	109.5
C(39)–C(40)–H(51)	109.5
H(49)–C(40)–H(51)	109.5
H(50)–C(40)–H(51)	109.5
O(8)–C(41)–O(7)	121.6(4)
O(8)–C(41)–C(42)	127.5(4)
O(7)–C(41)–C(42)	110.9(3)
C(41)–C(42)–C(43)	113.2(3)
C(41)–C(42)–H(52)	108.9
C(43)–C(42)–H(52)	108.9
C(41)–C(42)–H(53)	108.9
C(43)–C(42)–H(53)	108.9
H(52)–C(42)–H(53)	107.8
C(44)–C(43)–C(42)	112.7(3)
C(44)–C(43)–H(54)	109.1
C(42)–C(43)–H(54)	109.1
C(44)–C(43)–H(55)	109.1
C(42)–C(43)–H(55)	109.1
H(54)–C(43)–H(55)	107.8
C(45)–C(44)–C(43)	113.6(4)
C(45)–C(44)–H(56)	108.8
C(43)–C(44)–H(56)	108.8
C(45)–C(44)–H(57)	108.8
C(43)–C(44)–H(57)	108.8
H(56)–C(44)–H(57)	107.7
C(44)–C(45)–C(46)	115.2(4)
C(44)–C(45)–H(58)	108.5
C(46)–C(45)–H(58)	108.5
C(44)–C(45)–H(59)	108.5
C(46)–C(45)–H(59)	108.5
H(58)–C(45)–H(59)	107.5
C(47)–C(46)–C(45)	113.6(4)
C(47)–C(46)–H(60)	108.9

(*Continued*)

Table A3. Continued

C(45)–C(46)–H(60)	108.9
C(47)–C(46)–H(61)	108.9
C(45)–C(46)–H(61)	108.9
H(60)–C(46)–H(61)	107.7
C(46)–C(47)–C(48)	113.9(4)
C(46)–C(47)–H(62)	108.8
C(48)–C(47)–H(62)	108.8
C(46)–C(47)–H(63)	108.8
C(48)–C(47)–H(63)	108.8
H(62)–C(47)–H(63)	107.7
C(47)–C(48)–H(64)	109.5
C(47)–C(48)–H(65)	109.5
H(64)–C(48)–H(65)	109.5
C(47)–C(48)–H(66)	109.5
H(64)–C(48)–H(66)	109.5
H(65)–C(48)–H(66)	109.5

Table A4. Anisotropic displacement parameters ($Å^2 \times 10^3$) for PC7. The anisotropic displacement factor exponent takes the form: $-2\pi^2(h^2 a^{*2} U^{11} + \cdots + 2h\,k\,a^* b^* U^{12})$

	U^{11}	U^{22}	U^{33}	U^{23}	U^{13}	U^{12}
C(1)	31(2)	30(2)	31(2)	−13(2)	3(2)	−1(2)
C(2)	32(2)	24(2)	33(2)	−11(2)	−7(2)	−1(2)
C(3)	26(2)	20(2)	30(2)	−9(2)	4(2)	0(2)
C(4)	31(2)	17(2)	34(3)	−10(2)	6(2)	−6(2)
C(5)	30(2)	21(2)	33(3)	−6(2)	4(2)	−5(2)
C(6)	28(2)	22(2)	28(2)	−5(2)	2(2)	0(2)
C(7)	27(2)	21(2)	26(2)	−6(2)	5(2)	−1(2)
C(8)	29(2)	27(2)	32(2)	−11(2)	4(2)	−3(2)
C(9)	29(2)	22(2)	34(2)	−10(2)	1(2)	−1(2)
C(10)	27(2)	21(2)	30(2)	−8(2)	6(2)	−2(2)
C(11)	28(2)	21(2)	32(2)	−7(2)	5(2)	−2(2)
C(12)	34(2)	20(2)	32(2)	−3(2)	5(2)	−3(2)
C(13)	26(2)	25(2)	26(2)	−4(2)	1(2)	6(2)
C(14)	24(2)	25(2)	31(2)	−8(2)	0(2)	2(2)
C(15)	26(2)	21(2)	28(2)	−8(2)	4(2)	1(2)
C(16)	20(2)	24(2)	28(2)	−7(2)	2(2)	1(2)
O(1)	32(2)	17(1)	44(2)	−9(1)	1(1)	−4(1)
O(2)	33(2)	29(2)	46(2)	−14(1)	−3(1)	0(1)
O(3)	33(2)	27(2)	27(2)	−4(1)	−3(1)	−1(1)
O(4)	29(2)	75(2)	36(2)	−6(2)	3(1)	−1(2)
O(5)	34(2)	23(2)	35(2)	−8(1)	5(1)	−11(1)

(*Continued*)

Table A4. Continued

	U^{11}	U^{22}	U^{33}	U^{23}	U^{13}	U^{12}
O(6)	44(2)	49(2)	38(2)	−19(2)	5(2)	−14(2)
O(7)	33(2)	31(2)	29(2)	−3(1)	−2(1)	1(1)
O(8)	49(2)	77(3)	31(2)	−17(2)	−3(2)	15(2)
C(17)	44(3)	17(2)	29(2)	−4(2)	6(2)	−1(2)
C(18)	34(2)	20(2)	44(3)	−6(2)	−1(2)	−8(2)
C(19)	36(2)	29(2)	41(3)	−9(2)	−2(2)	−5(2)
C(20)	39(3)	36(3)	37(3)	−12(2)	−1(2)	−4(2)
C(21)	44(3)	60(3)	40(3)	−8(3)	−6(2)	−13(3)
C(22)	56(3)	50(3)	46(3)	−5(3)	−5(3)	−9(3)
C(23)	80(4)	67(4)	46(3)	−9(3)	−12(3)	−12(3)
C(24)	116(5)	50(3)	43(3)	−6(3)	4(3)	−16(3)
C(25)	35(3)	26(2)	28(3)	−7(2)	0(2)	2(2)
C(26)	37(2)	32(2)	29(2)	−5(2)	−2(2)	−1(2)
C(27)	43(3)	35(3)	33(3)	−4(2)	−2(2)	−9(2)
C(28)	40(3)	28(2)	35(3)	−6(2)	−2(2)	−5(2)
C(29)	42(3)	34(3)	34(3)	−4(2)	−1(2)	−5(2)
C(30)	42(3)	33(2)	32(3)	−6(2)	−3(2)	−7(2)
C(31)	48(3)	35(3)	35(3)	−5(2)	0(2)	−5(2)
C(32)	71(3)	38(3)	39(3)	−4(2)	−6(3)	−11(3)
C(33)	26(2)	24(2)	38(3)	−6(2)	0(2)	−5(2)
C(34)	40(3)	25(2)	37(3)	−6(2)	−1(2)	−5(2)
C(35)	39(3)	22(2)	47(3)	−8(2)	3(2)	−7(2)
C(36)	39(3)	35(3)	44(3)	−5(2)	1(2)	0(2)
C(37)	55(3)	28(3)	50(3)	−7(2)	−5(2)	2(2)
C(38)	65(3)	29(3)	48(3)	−10(2)	−6(3)	0(2)
C(39)	64(3)	30(3)	51(3)	−3(2)	5(3)	1(3)
C(40)	87(4)	53(3)	52(3)	−8(3)	2(3)	1(3)
C(41)	35(2)	27(2)	33(3)	−2(2)	−6(2)	1(2)
C(42)	27(2)	32(2)	35(3)	−6(2)	−1(2)	−2(2)
C(43)	42(3)	31(2)	33(3)	−2(2)	−5(2)	−3(2)
C(44)	35(2)	32(2)	39(3)	−4(2)	0(2)	−3(2)
C(45)	37(2)	28(2)	37(3)	−3(2)	−3(2)	−2(2)
C(46)	38(3)	30(2)	40(3)	−8(2)	−5(2)	−1(2)
C(47)	42(3)	31(3)	42(3)	−2(2)	−3(2)	−4(2)
C(48)	65(3)	41(3)	40(3)	0(2)	−10(3)	2(3)

Table A5. Atomic coordinates ($\times 10^4$) and equivalent isotropic displacement parameters ($Å^2 \times 10^3$) for PC9. U(eq) is defined as one third of the trace of the orthogonalized U^{ij} tensor

	x	*y*	*z*	U(eq)
C(1)	3892(5)	839(5)	3289(12)	53(2)
C(2)	4571(5)	1128(5)	3466(12)	52(2)
C(3)	5325(6)	789(5)	1902(12)	50(2)
C(4)	6049(6)	1073(5)	1953(14)	57(2)
C(5)	6776(6)	730(5)	451(13)	57(2)
C(6)	6805(5)	110(4)	−1253(12)	50(2)
C(7)	6098(5)	−193(4)	−1512(12)	48(2)
C(8)	5362(5)	151(4)	85(12)	48(2)
O(1)	6011(4)	1704(3)	3690(9)	59(1)
O(2)	4941(5)	2799(4)	1133(10)	80(2)
C(9)	5374(6)	2568(5)	3127(16)	60(2)
C(10)	5262(6)	3161(5)	5280(13)	59(2)
C(11)	4344(6)	4022(5)	5030(14)	60(2)
C(12)	4207(6)	4664(5)	7115(14)	59(2)
C(13)	3291(6)	5530(5)	6904(14)	61(2)
C(14)	3151(6)	6156(5)	9004(13)	55(2)
C(15)	2258(6)	7037(5)	8795(16)	69(2)
C(16)	2090(7)	7624(6)	10,963(16)	70(2)
C(17)	1190(7)	8499(6)	10,732(18)	76(2)
C(18)	1016(7)	9076(6)	12,970(18)	84(3)
O(3)	7534(4)	−237(3)	−2868(9)	58(1)
O(4)	8433(6)	−1321(6)	−161(13)	132(4)
C(19)	8329(6)	−1009(6)	−2142(17)	69(2)
C(20)	8978(7)	−1417(6)	−4161(14)	68(2)
C(21)	9390(6)	−2425(5)	−4062(14)	65(2)
C(22)	10,050(6)	−2892(5)	−6087(13)	61(2)
C(23)	10,432(7)	−3903(5)	−6020(15)	69(2)
C(24)	11,045(6)	−4388(5)	−8020(14)	62(2)
C(25)	11,405(6)	−5386(6)	−7954(15)	68(2)
C(26)	12,024(6)	−5903(5)	−9960(14)	65(2)
C(27)	12,347(7)	−6888(6)	−9926(16)	78(3)
C(28)	12,970(8)	−7414(6)	−11,897(15)	79(3)

Table A6. Bond lengths (Å) and angles (°) for PC9

C(1)–C(2)	1.356(9)
C(1)–C(7)#1	1.427(8)
C(1)–H(1)	0.9500
C(2)–C(3)	1.408(10)
C(2)–H(2)	0.9500
C(3)–C(4)	1.420(10)
C(3)–C(8)	1.423(9)
C(4)–C(5)	1.356(10)
C(4)–O(1)	1.383(8)
C(5)–C(6)	1.362(9)
C(5)–H(3)	0.9500
C(6)–O(3)	1.400(8)
C(6)–C(7)	1.415(9)
C(7)–C(8)	1.401(10)
C(7)–C(1)#1	1.427(8)
C(8)–C(8)#1	1.438(13)
O(1)–C(9)	1.354(10)
O(2)–C(9)	1.196(10)
C(9)–C(10)	1.485(10)
C(10)–C(11)	1.494(11)
C(10)–H(4)	0.9900
C(10)–H(5)	0.9900
C(11)–C(12)	1.503(9)
C(11)–H(6)	0.9900
C(11)–H(7)	0.9900
C(12)–C(13)	1.497(11)
C(12)–H(8)	0.9900
C(12)–H(9)	0.9900
C(13)–C(14)	1.492(9)
C(13)–H(10)	0.9900
C(13)–H(11)	0.9900
C(14)–C(15)	1.492(11)
C(14)–H(12)	0.9900
C(14)–H(13)	0.9900
C(15)–C(16)	1.478(11)
C(15)–H(14)	0.9900
C(15)–H(15)	0.9900
C(16)–C(17)	1.493(13)
C(16)–H(16)	0.9900
C(16)–H(17)	0.9900
C(17)–C(18)	1.498(12)
C(17)–H(18)	0.9900
C(17)–H(19)	0.9900
C(18)–H(20)	0.9800
C(18)–H(21)	0.9800

(*Continued*)

Table A6. Continued

C(18)–H(22)	0.9800
O(3)–C(19)	1.355(10)
O(4)–C(19)	1.178(11)
C(19)–C(20)	1.494(11)
C(20)–C(21)	1.514(11)
C(20)–H(23)	0.9900
C(20)–H(24)	0.9900
C(21)–C(22)	1.521(10)
C(21)–H(25)	0.9900
C(21)–H(26)	0.9900
C(22)–C(23)	1.522(11)
C(22)–H(27)	0.9900
C(22)–H(28)	0.9900
C(23)–C(24)	1.480(11)
C(23)–H(29)	0.9900
C(23)–H(30)	0.9900
C(24)–C(25)	1.505(11)
C(24)–H(31)	0.9900
C(24)–H(32)	0.9900
C(25)–C(26)	1.500(11)
C(25)–H(33)	0.9900
C(25)–H(34)	0.9900
C(26)–C(27)	1.494(12)
C(26)–H(35)	0.9900
C(26)–H(36)	0.9900
C(27)–C(28)	1.493(12)
C(27)–H(37)	0.9900
C(27)–H(38)	0.9900
C(28)–H(39)	0.9800
C(28)–H(40)	0.9800
C(28)–H(41)	0.9800
C(2)–C(1)–C(7)#1	121.9(6)
C(2)–C(1)–H(1)	119.1
C(7)#1–C(1)–H(1)	119.1
C(1)–C(2)–C(3)	120.7(6)
C(1)–C(2)–H(2)	119.6
C(3)–C(2)–H(2)	119.6
C(2)–C(3)–C(4)	123.7(6)
C(2)–C(3)–C(8)	119.6(6)
C(4)–C(3)–C(8)	116.6(7)
C(5)–C(4)–O(1)	120.1(7)
C(5)–C(4)–C(3)	122.8(6)
O(1)–C(4)–C(3)	117.1(6)
C(4)–C(5)–C(6)	119.6(7)
C(4)–C(5)–H(3)	120.2

(*Continued*)

Table A6. Continued

C(6)–C(5)–H(3)	120.2
C(5)–C(6)–O(3)	120.7(6)
C(5)–C(6)–C(7)	122.0(6)
O(3)–C(6)–C(7)	117.3(6)
C(8)–C(7)–C(6)	117.9(6)
C(8)–C(7)–C(1)#1	118.8(6)
C(6)–C(7)–C(1)#1	123.2(6)
C(7)–C(8)–C(3)	121.0(6)
C(7)–C(8)–C(8)#1	119.8(7)
C(3)–C(8)–C(8)#1	119.2(8)
C(9)–O(1)–C(4)	116.7(6)
O(2)–C(9)–O(1)	122.4(7)
O(2)–C(9)–C(10)	125.5(7)
O(1)–C(9)–C(10)	112.0(7)
C(9)–C(10)–C(11)	113.0(6)
C(9)–C(10)–H(4)	109.0
C(11)–C(10)–H(4)	109.0
C(9)–C(10)–H(5)	109.0
C(11)–C(10)–H(5)	109.0
H(4)–C(10)–H(5)	107.8
C(10)–C(11)–C(12)	115.4(6)
C(10)–C(11)–H(6)	108.4
C(12)–C(11)–H(6)	108.4
C(10)–C(11)–H(7)	108.4
C(12)–C(11)–H(7)	108.4
H(6)–C(11)–H(7)	107.5
C(13)–C(12)–C(11)	116.3(6)
C(13)–C(12)–H(8)	108.2
C(11)–C(12)–H(8)	108.2
C(13)–C(12)–H(9)	108.2
C(11)–C(12)–H(9)	108.2
H(8)–C(12)–H(9)	107.4
C(14)–C(13)–C(12)	116.0(6)
C(14)–C(13)–H(10)	108.3
C(12)–C(13)–H(10)	108.3
C(14)–C(13)–H(11)	108.3
C(12)–C(13)–H(11)	108.3
H(10)–C(13)–H(11)	107.4
C(13)–C(14)–C(15)	116.9(6)
C(13)–C(14)–H(12)	108.1
C(15)–C(14)–H(12)	108.1
C(13)–C(14)–H(13)	108.1
C(15)–C(14)–H(13)	108.1
H(12)–C(14)–H(13)	107.3
C(16)–C(15)–C(14)	116.5(7)

(*Continued*)

Table A6. Continued

C(16)–C(15)–H(14)	108.2
C(14)–C(15)–H(14)	108.2
C(16)–C(15)–H(15)	108.2
C(14)–C(15)–H(15)	108.2
H(14)–C(15)–H(15)	107.3
C(15)–C(16)–C(17)	115.8(8)
C(15)–C(16)–H(16)	108.3
C(17)–C(16)–H(16)	108.3
C(15)–C(16)–H(17)	108.3
C(17)–C(16)–H(17)	108.3
H(16)–C(16)–H(17)	107.4
C(16)–C(17)–C(18)	115.2(8)
C(16)–C(17)–H(18)	108.5
C(18)–C(17)–H(18)	108.5
C(16)–C(17)–H(19)	108.5
C(18)–C(17)–H(19)	108.5
H(18)–C(17)–H(19)	107.5
C(17)–C(18)–H(20)	109.5
C(17)–C(18)–H(21)	109.5
H(20)–C(18)–H(21)	109.5
C(17)–C(18)–H(22)	109.5
H(20)–C(18)–H(22)	109.5
H(21)–C(18)–H(22)	109.5
C(19)–O(3)–C(6)	116.4(6)
O(4)–C(19)–O(3)	121.2(8)
O(4)–C(19)–C(20)	126.3(8)
O(3)–C(19)–C(20)	112.4(7)
C(19)–C(20)–C(21)	109.7(7)
C(19)–C(20)–H(23)	109.7
C(21)–C(20)–H(23)	109.7
C(19)–C(20)–H(24)	109.7
C(21)–C(20)–H(24)	109.7
H(23)–C(20)–H(24)	108.2
C(20)–C(21)–C(22)	113.0(7)
C(20)–C(21)–H(25)	109.0
C(22)–C(21)–H(25)	109.0
C(20)–C(21)–H(26)	109.0
C(22)–C(21)–H(26)	109.0
H(25)–C(21)–H(26)	107.8
C(21)–C(22)–C(23)	112.4(6)
C(21)–C(22)–H(27)	109.1
C(23)–C(22)–H(27)	109.1
C(21)–C(22)–H(28)	109.1
C(23)–C(22)–H(28)	109.1
H(27)–C(22)–H(28)	107.8

(*Continued*)

Table A6. Continued

C(24)–C(23)–C(22)	114.8(7)
C(24)–C(23)–H(29)	108.6
C(22)–C(23)–H(29)	108.6
C(24)–C(23)–H(30)	108.6
C(22)–C(23)–H(30)	108.6
H(29)–C(23)–H(30)	107.5
C(23)–C(24)–C(25)	114.2(7)
C(23)–C(24)–H(31)	108.7
C(25)–C(24)–H(31)	108.7
C(23)–C(24)–H(32)	108.7
C(25)–C(24)–H(32)	108.7
H(31)–C(24)–H(32)	107.6
C(26)–C(25)–C(24)	115.9(7)
C(26)–C(25)–H(33)	108.3
C(24)–C(25)–H(33)	108.3
C(26)–C(25)–H(34)	108.3
C(24)–C(25)–H(34)	108.3
H(33)–C(25)–H(34)	107.4
C(27)–C(26)–C(25)	115.4(7)
C(27)–C(26)–H(35)	108.4
C(25)–C(26)–H(35)	108.4
C(27)–C(26)–H(36)	108.4
C(25)–C(26)–H(36)	108.4
H(35)–C(26)–H(36)	107.5
C(28)–C(27)–C(26)	116.0(8)
C(28)–C(27)–H(37)	108.3
C(26)–C(27)–H(37)	108.3
C(28)–C(27)–H(38)	108.3
C(26)–C(27)–H(38)	108.3
H(37)–C(27)–H(38)	107.4
C(27)–C(28)–H(39)	109.5
C(27)–C(28)–H(40)	109.5
H(39)–C(28)–H(40)	109.5
C(27)–C(28)–H(41)	109.5
H(39)–C(28)–H(41)	109.5
H(40)–C(28)–H(41)	109.5

Symmetry transformations used to generate equivalent atoms: #1 $-x+1, -y, -z$.

Table A7. Anisotropic displacement parameters ($Å^2 \times 10^3$) for PC9. The anisotropic displacement factor exponent takes the form: $-2\pi^2(h^2\, a^{*2}U^{11} + \cdots + 2\,h\,k\,a^*b^*U^{12})$

	U^{11}	U^{22}	U^{33}	U^{23}	U^{13}	U^{12}
C(1)	65(5)	52(4)	55(4)	−19(3)	27(3)	−34(4)
C(2)	66(5)	45(4)	47(4)	−10(3)	14(3)	−27(4)
C(3)	72(5)	42(4)	41(3)	−5(3)	13(3)	−31(4)
C(4)	65(5)	48(4)	64(5)	−18(4)	21(4)	−29(4)
C(5)	77(6)	55(4)	55(4)	−10(4)	24(4)	−42(4)
C(6)	59(5)	43(4)	49(4)	−1(3)	22(3)	−21(3)
C(7)	52(4)	45(4)	46(4)	−9(3)	8(3)	−21(3)
C(8)	62(5)	40(3)	44(4)	−9(3)	14(3)	−24(3)
O(1)	67(3)	59(3)	51(3)	−20(2)	9(2)	−30(3)
O(2)	131(6)	52(3)	48(3)	−3(3)	−9(3)	−37(3)
C(9)	72(6)	40(4)	78(6)	−20(4)	19(4)	−32(4)
C(10)	74(6)	53(4)	51(4)	−7(3)	1(4)	−31(4)
C(11)	72(5)	48(4)	60(4)	−7(3)	12(4)	−27(4)
C(12)	67(5)	52(4)	57(4)	−10(4)	6(4)	−27(4)
C(13)	66(5)	54(4)	63(5)	−12(4)	10(4)	−29(4)
C(14)	63(5)	52(4)	48(4)	−8(3)	6(3)	−26(4)
C(15)	69(6)	49(4)	78(5)	−18(4)	8(4)	−18(4)
C(16)	84(6)	63(5)	73(5)	−19(4)	16(4)	−42(5)
C(17)	67(6)	57(5)	96(6)	−18(4)	7(5)	−24(4)
C(18)	90(7)	52(5)	106(7)	−14(5)	27(5)	−28(5)
O(3)	61(3)	57(3)	59(3)	−9(2)	24(2)	−28(3)
O(4)	115(6)	124(7)	59(4)	3(4)	23(4)	29(5)
C(19)	56(5)	65(5)	65(5)	−19(4)	13(4)	−9(4)
C(20)	77(6)	66(5)	57(4)	−11(4)	16(4)	−29(5)
C(21)	64(5)	64(5)	66(5)	−17(4)	21(4)	−27(4)
C(22)	72(5)	61(4)	46(4)	−13(4)	14(3)	−28(4)
C(23)	77(6)	60(5)	71(5)	−18(4)	25(4)	−31(5)
C(24)	63(5)	55(4)	64(5)	−17(4)	11(4)	−24(4)
C(25)	76(6)	65(5)	68(5)	−16(4)	25(4)	−35(5)
C(26)	73(6)	66(5)	58(4)	−16(4)	15(4)	−31(4)
C(27)	86(7)	63(5)	71(5)	−13(4)	22(4)	−20(5)
C(28)	107(8)	66(5)	57(5)	−11(4)	19(4)	−33(5)

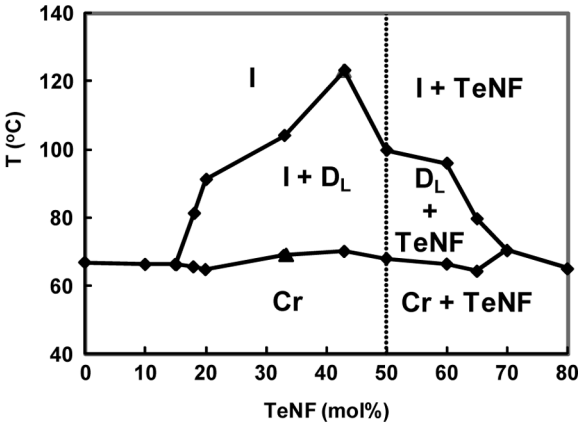

(a)

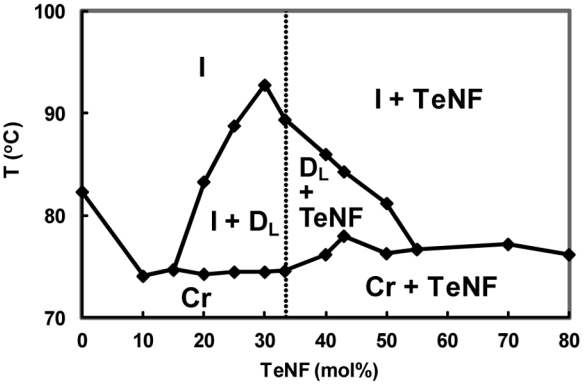

(b)

Figure A1. The binary phase diagrams for (a) PC9-TeNF and (b) PC15-TeNF systems.